# Super-Resolution Chemical Imaging with Plasmonic Substrates

Aeli P. Olson,[†] Christopher T. Ertsgaard,[†] Sarah N. Elliott,[†] and Nathan C. Lindquist*

Physics Department, Bethel University, St. Paul, Minnesota 55112, United States

**S** *Supporting Information*

**ABSTRACT:** We demonstrate super-resolution chemical imaging with plasmonic nanoholes via surface-enhanced Raman spectroscopy (SERS). Due to large field enhancements, blinking behavior of SERS hot spots was observed and processed using a stochastic optical reconstruction microscopy (STORM) algorithm. This enabled localization to within 10 nm and high-resolution imaging. However, illumination of the sample with a static laser beam produced only SERS hot spots in fixed locations, leaving noticeable gaps in the final images. By randomly altering the phase profile of the incident beam with a simple optical diffuser, the hot spots were shifted across the plasmonic surface to illuminate different areas of the sample, thereby rendering a final image without the gaps. A tunable band-pass filter was used to preserve spectral information, allowing chemical contrast imaging. Images were then compared to those obtained with a scanning electron microscope. Finally, we show that super-resolution SERS images can also be obtained with our dynamic illumination technique on even the most basic plasmonic substrate: as-deposited rough silver films. These results show significant potential for the use of simple plasmonic substrates with straightforward illumination and collection schemes for super-resolution chemical imaging.

**KEYWORDS:** *plasmonics, surface-enhanced Raman spectroscopy (SERS), stochastic optical reconstruction microscopy (STORM), super-resolution imaging, chemical imaging*
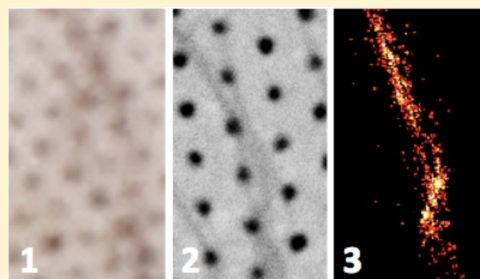
Diffraction limits the resolution of standard optical microscopy and hinders many of the most demanding applications in imaging and spectroscopy. Given its broad significance, much effort has been spent toward developing super-resolution optical imaging.[1−4] While various techniques exist using fluorescent tags, options that do not use fluorescence labels would also be particularly useful.[5] Furthermore, gathering spectral information via Raman spectroscopy would allow super-resolution chemical contrast imaging.[6] As one particular solution toward this goal,[7] the field of plasmonics[8−10] aims to manipulate light within dimensions much smaller than the optical wavelength by exploiting surface plasmon resonances in metallic nanostructures. Plasmons are oscillations of the conduction electrons at the surface of a metal and can squeeze or focus electromagnetic energy into very small volumes. These locally enhanced fields, sometimes called "hot spots", can be used for biosensing applications,[11−14] surface-enhanced Raman spectroscopy (SERS),[15−19] tip-enhanced imaging,[20] or nanotweezing.[21,22] Hot spots have also been used to optically map metallic nanostructures[7,23,24] or to image biological structures[25] via SERS and with subdiffraction-limited resolution.[26] However, using SERS for wide-field imaging requires uniform and dense hot spot generation. Unfortunately, due to the inhomogeneous and often random nature of hot spot generation,[19] this remains a significant challenge. To address this, some level of control of these hot spots would provide many benefits. While focused plasmons have been shifted across a plasmonic surface via dynamic illumination,[29,30] SERS imaging with these techniques has not been fully explored. Likewise, SERS has not been exploited to gather chemical information in various other plasmonic super-resolution imaging techniques such as plasmonic structured illumination microscopy[31−33] and spatially activated plasmonic hot spot imaging.[34] We previously reported on the use of a spatial light modulator (SLM) to dynamically shift SERS hot spots with subdiffraction-limited resolution.[27] In particular, that work gave an experimental demonstration of localizing and shifting a single SERS hot spot with <100 nm precision in and around a single nanohole. Shifting the location of hot spots over a surface to illuminate different regions of a sample suggested significant potential for imaging purposes and has been in continuous development.[28,35] In this paper, we demonstrate super-resolution chemical imaging using this dynamic illumination technique with two different plasmonic substrates: nanohole arrays and as-deposited rough silver films. Due to the large field enhancements from these plasmonic hot spots, blinking behavior of the SERS was observed and processed using either a custom stochastic optical reconstruction microscopy (STORM) algorithm[36] or the open-source alternative rapid-STORM.[37] This enabled super-resolution SERS-STORM chemical imaging. Importantly, our optical images are compared to scanning electron microscope (SEM) images and, by using a tunable band-pass filter, are analyzed to display chemical contrast. Finally, we demonstrate the ability to dynamically shift these hot spots—static illumination typically produces nonuniform static hot spots that leave gaps in the
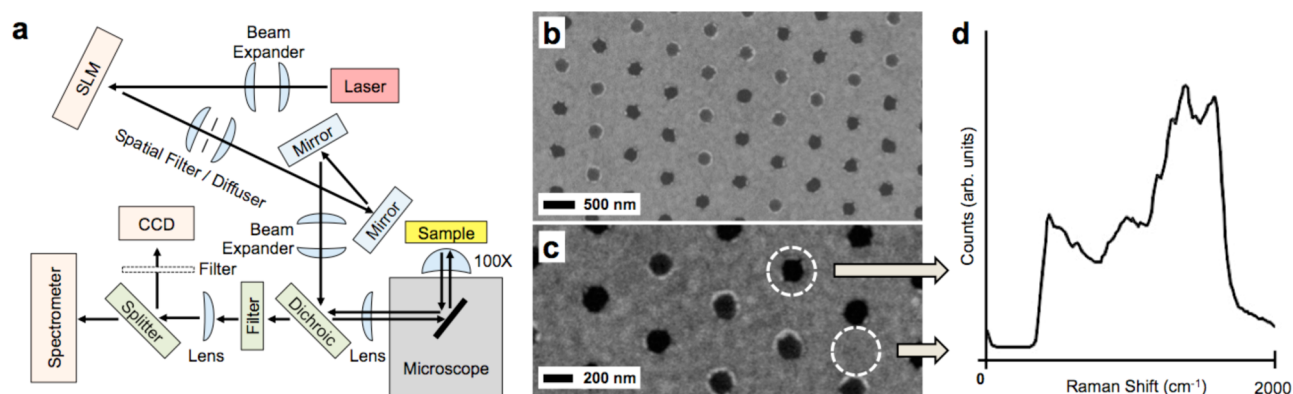
**Figure 1.** Experimental setup and nanohole chips. (a) Schematic of the microscope system. In some experiments, an optical diffuser was used to alter the phase profile of the laser beam instead of the SLM. The reflected light passes through a long-pass filter and is sent to either a spectrometer or a CCD camera for imaging. A tunable filter also provides spectral selectivity. (b) SEM image of the nanohole chips used for SERS and imaging experiments. (c) The 50 nm thick silver film had small random grain boundaries in between the nanoholes that also produced SERS signals. (d) Representative SERS spectrum of a strand of collagen fiber that was deposited onto the nanohole surface.
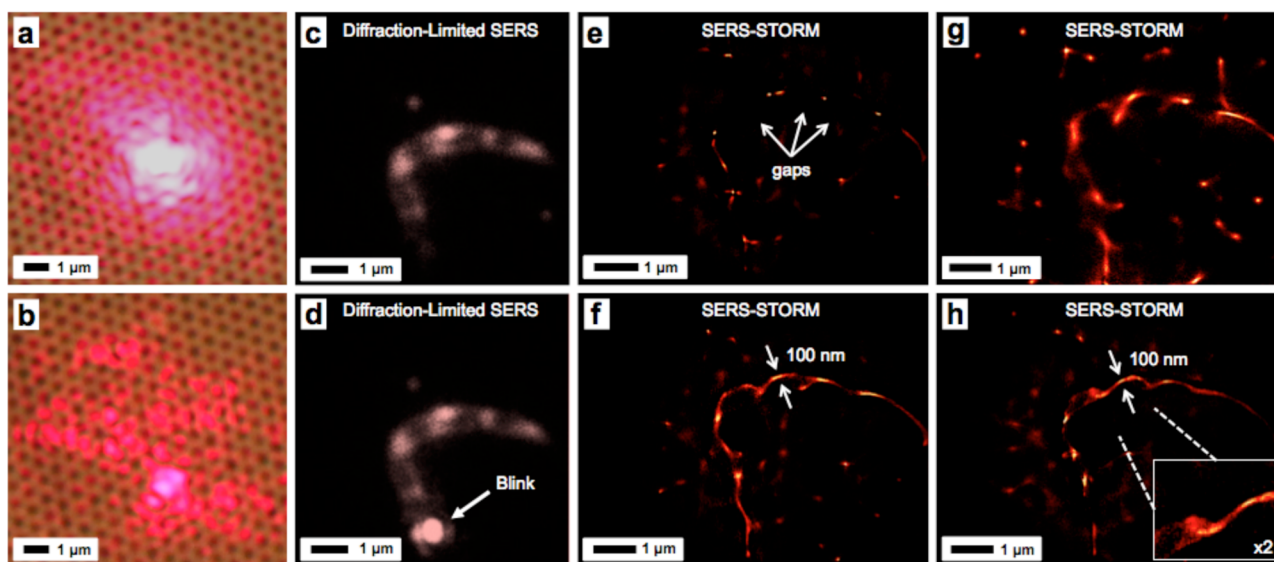


**Figure 2.** Super-resolution images of a collagen fiber strand with various illumination schemes. (a) Bright-field optical micrograph of the nanohole array with uniform Gaussian illumination. (b) Bright-field optical micrograph of a "random" illumination profile by illuminating through an optical diffuser. Moving the diffuser changes the pattern. (c) Single frame of the SERS substrate as imaged on the CCD camera. (d) The SERS hot spots are seen to "blink" in time, allowing the use of a STORM fitting process to build up a final image. (e) Illumination of the sample with a static beam profile, processed with a SERS-STORM technique. Many gaps are seen with static illumination of the sample. (f) Holographic illumination with the SLM but randomly shifting the phase profile. The gaps are now filled in, producing a full super-resolution image. (g) Holographic illumination with a striped grating pattern while dynamically shifting the angle (similar to techniques used in structured illumination microscopy[42]). There was more noise in the image and lower resolution, but the fiber pattern is still apparent. (h) Illumination with an unfocused laser beam shining through a moving diffuser, mimicking the dynamic random phase mask of the SLM. This random diffuser technique replicated that of the SLM. (Inset) More detail of a portion of the fiber.

final image—by moving an optical diffuser around in the beam path during the SERS-STORM imaging process, fully replacing the SLM. In general, SERS substrates suffer from nonuniform enhancements, and significant effort has gone into their optimization.[19] Our illumination techniques may help overcome this limitation, without necessitating the redesign of a given substrate itself but by instead tailoring the illumination profile. Ideally, both a SERS substrate and its illumination profile could be optimized for wide-field, uniform, super-resolution SERS imaging. In any case, random illumination through a moving optical diffuser eliminates the need to solve a difficult inverse problem for specifically tailored hot spot patterns[29,30] or the need for an expensive SLM. This research

also suggests a final improvement, discussed further below, that perhaps even a randomly patterned SERS substrate with random illumination could also be used for uniform, super-resolution imaging.

## ■ RESULTS AND DISCUSSION

For our plasmonic substrates, we used either a 700 nm periodicity hexagonal array of 200 nm diameter holes through a 50 nm thick silver film or an as-deposited 10 nm thick silver film on a silicon wafer. Nanohole arrays cause enhanced transmission effects[38] and have been used widely for biosensing[13] as well as SERS,[17] while the random roughness of a thin as-deposited silver film can also excite SERS. Changing
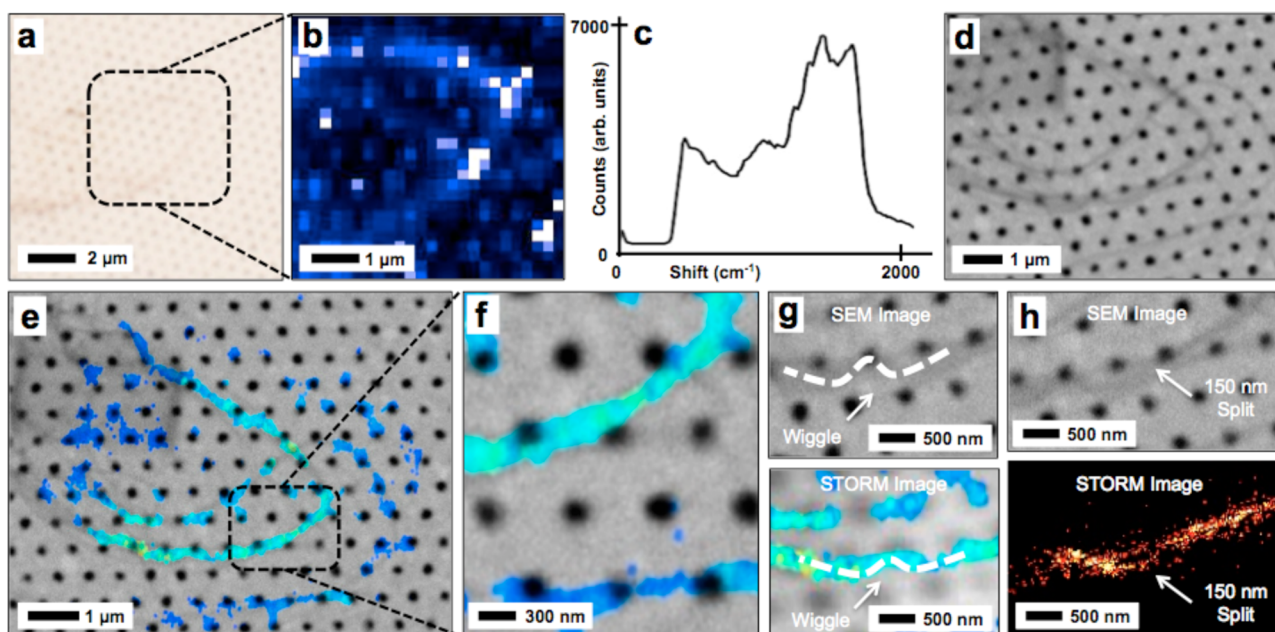
**Figure 3.** Super-resolution imaging of collagen fibrils on a hexagonal silver nanohole array. (a) Bright-field image of collagen fibers taken with a CCD camera through a 100× microscope objective. (b) Scanning a laser and monitoring (c) the intensity of the SERS peak at 1500 cm$^{-1}$ produces a chemical map of the fiber with a resolution limited by the size of the focused laser spot. This is the same SERS spectrum shown in Figure 1, reproduced here for convenience. A scanning geometry collected a full SERS spectrum at each point and thus contains information for both a diffraction-limited SERS image and a chemical contrast image. Our SERS-STORM imaging technique aims to maintain the chemical contrast shown in (c) while improving the spatial resolution shown in (b). (d) SEM image of the same collagen strand. (e) Overlay of a SERS-STORM image and the same SEM image. (f) The SERS-STORM imaging technique reproduces the fine features of the strand, seen to traverse between the nanoholes and, in other regions, (g) to have small curves and (h) splits.

the illumination profile allows us to shift the plasmonic hot spots in and around the array for dynamic imaging and hot spot placement.[27] Figure 1a shows a schematic of the microscope illumination system with a 660 nm laser (Laser Quantum) and a phase-only SLM (Hamamatsu). The sample is mounted on a nanopositioning stage (Mad City Labs) for precise alignment. With a proper pattern and a spatial filter, the SLM is capable of illuminating the sample with a controlled amplitude and phase[39] for subwavelength hot spot placement.[27] In our current case, however, the SLM was used to display only random illumination profiles and was later even replaced with an optical diffuser placed at the position of the spatial filter as described below. Reflected light passed through a long-pass filter (Semrock) and could be sent to a spectrometer or to an electron multiplied (EM) CCD (PCO). In some experiments, the Raman light would also pass through a tunable band-pass filter (Semrock) before arriving at the EM-CCD. For chemical imaging, we examined the SERS signals from strands of type I collagen protein fiber adsorbed on the silver surface as well as microcontact printed patterns of hexadecanethiol or background layers of methylbenzenethiol. A SEM image of the nanohole sample is shown in Figure 1b. The texturing in between the nanoholes is apparent in a zoomed-in view (Figure 1c). Since this substrate is used for imaging, this texturing is important to also enable SERS between the nanoholes.

A template stripping method was used to produce the silver nanohole arrays[40] with a commercially available silicon template (LightSmyth). The substrates were then coated with collagen protein fibers, hexadecanethiol, or methylbenzenethiol. The samples were then illuminated with the laser. The illumination profile was either a uniform unfocused Gaussian beam (Figure 2a) or a random, speckled pattern from the SLM

or an optical diffuser (Figure 2b). Changing the illumination profile will change the location of the SERS hot spots. Due to the large plasmonic field enhancement of the nanoholes, the SERS signal would "blink" in time, allowing us to perform a super-resolution SERS-STORM imaging process.[25] Two frames from the EM-CCD camera show the blinking behavior of a single collagen strand (Figure 2c,d). As the SERS hot spots blink in time, they can be localized,[16] eventually forming a full image.[25] In our case, most data sets were analyzed with rapidSTORM, an open-source software program that localized the blinks.[37] We also made use of custom MATLAB code from our previous publication[27] as verification. To minimize the effect of the background signal, only "blinks" above a certain threshold were used for imaging purposes, set as a parameter in the rapidSTORM software. While blinking is typically associated with random diffusion of molecules in and out of hot spots, the blinking behavior of the collagen strands seen here is perhaps due to random vibrations of the strands that were adsorbed to the silver surface. See the Supporting Information Video S1 for some sample data of a "blinking" collagen strand.

Figure 2e−h show the effect on the final image quality of shifting the SERS hot spots with various techniques. We first illuminated a nanohole array surface with an area that contained a ~5 μm long collagen fibril. The SERS signal from this fiber showed blinking behavior (Figure 2c, d) and was therefore suitable for SERS-STORM analysis. For Figure 2, we used rapidSTORM with a threshold specified that minimized the background signal. With a static ~10 μm wide illumination beam and after collecting ~1500 frames over several minutes, the resulting SERS-STORM images had considerable "gaps" (Figure 2e). This indicated that the plasmonic hot spots were
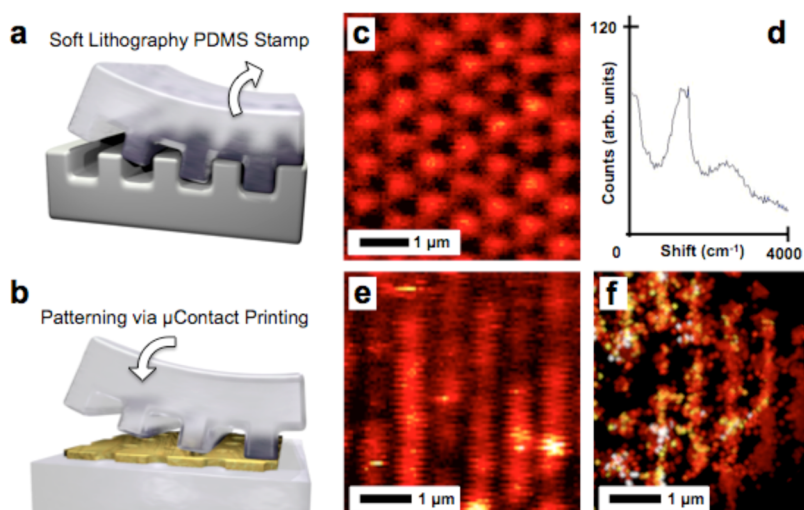
**Figure 4.** Super-resolution imaging of a chemical pattern. (a) Soft lithography is used to produce a PDMS stamp for (b) microcontact printing of hexadecanethiol stripes. The stamp is a linear stripe grating with an 800 nm period. (c) Scanning the laser over the surface reveals an optical reflection image of the nanoholes. (d) Monitoring the SERS intensity at 2500 cm$^{-1}$ reveals (e) a diffraction-limited image of the chemical stripe pattern formed via microcontact printing. (f) On a similar sample of methylbenzenethiol, these stripes can also be imaged via our SERS-STORM technique, revealing finer features of the chemical pattern.

not uniform and were unable to illuminate the entire strand. The SLM was then programmed to change the illuminating profile randomly, producing a "speckled" pattern as in Figure 2b. This created random placement of the hot spots over the illumination area. By randomly shuffling the speckle pattern every 100 frames with the same total number of frames as before, better imaging was achieved by filling in these gaps (Figure 2f). In this case, the collagen fibril is observed to be around 100 nm thick, consistent with previous observations[41] and smaller than the diffraction-limited resolution of our microscope. Therefore, the use of the SLM to randomly shift the SERS hot spots was critical for reducing the presence of large gaps in the images. We also tried a randomly rotating stripe pattern as the illumination profile. After collecting 1500 frames of blinking and shifting SERS signals, the strand was "filled in" as before (Figure 2g). The stripe patterns (~1 $\mu$m period) illuminated a larger area for the same overall beam power and therefore had more noise in the final image. Finally, if a similar effect could be reproduced through less expensive and specialized means, our technique could then be more readily available, accessible, and reproducible. To explore this, fully replacing the SLM, a lightly scuffed plastic disk diffuser was used and randomly moved about by hand in the path of the illuminating laser beam shown in Figure 1. This happened during the STORM imaging process. This randomly shifting illumination profile also replicated a detailed STORM image of the same collagen strand (Figure 2h).

Figure 2 shows that while the background noise varies in each illumination technique, the collagen fiber is well reproduced. Indeed, it appears as if illumination through a randomly shifting optical diffuser produced one of the best images (Figure 2h). Our results show that random, speckled illumination patterns are sufficient to fill in the gaps for SERS imaging. Therefore, random illumination through a diffuser, instead of via the SLM (a single frame of the speckle pattern is shown in Figure 2b), is sufficient if the diffuser randomly shifts, rotates, or moves during the STORM imaging process. This suggests that the illumination need not be tailored to the specific metallic nanosurface as long as the illumination

includes a dynamic component to fill in the SERS hot spots and the final SERS-STORM images. This opens up the possibility, explored further below, that other plasmonic substrates may also be suitable for similar SERS-STORM imaging, namely, a randomly roughened, as-deposited silver surface in place of the nanoholes.

Figure 3 demonstrates the accuracy of our imaging technique. Initially, it is not clear that using a basic STORM algorithm to localize each blinking event would produce an accurate replication of the sample. For example, the blinking and localization from the collagen fiber molecules may be coupling and interfering with neighboring hot spots, shifting the apparent location of the signals from their original positions.[43] To explore this possibility, Figure 3 depicts a SERS-STORM image of another collagen fiber sample with an SEM image of the same area. The same collagen strand was imaged four different ways (SERS-STORM, laser scanning SERS, bright-field imaging, and SEM). The image of the strand in Figure 3a is a bright-field optical micrograph, showing the nanohole array with extremely faint collagen strands running around the surface. The image in Figure 3b was constructed by monitoring the intensities of the SERS signal as a tightly focused laser was scanned over the surface with the nanopositioning stage. A chemical map is formed by plotting the intensity of a particular region of the SERS spectrum, e.g., ~1500 cm$^{-1}$ in Figure 3c, corresponding to the $\nu$(C=O) stretching mode of the protein. The curved collagen strand is seen, although the SERS intensity varies from pixel to pixel due to the blinking effect or nonuniform hot spot generation. It is the chemical contrast of Figure 3c we aim to replicate with our SERS-STORM chemical imaging technique while at the same time improving the spatial resolution of Figure 3b. Figure 3d shows the SEM image of the same area, clearly showing the collagen strands. This time, the strand is seen to weave in and around the nanoholes, features that are not entirely resolvable in the diffraction-limited optical images. Figure 3e shows the SERS-STORM image overlaid with the SEM image. The SERS image accurately reproduces the curvature (Figure 3f) and fine features (Figure 3g) captured by the SEM. Figure 3h shows a
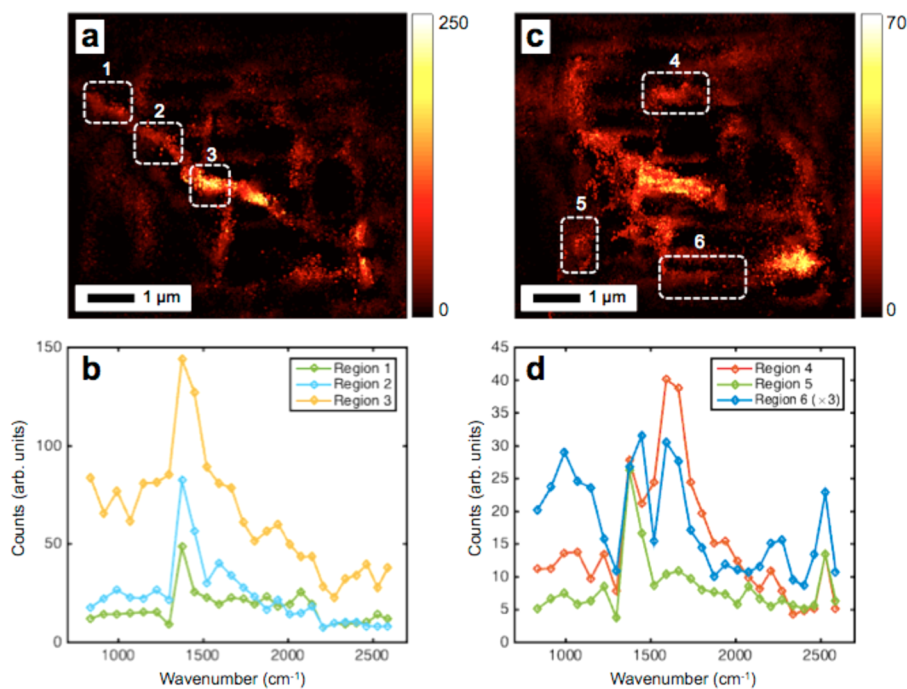
**Figure 5.** Chemical contrast imaging with SERS-STORM using a tunable band-pass filter. (a) Image of a collagen fibril with the band-pass filter tuned to enhance the strand. In this case, the silver nanohole chip was also incubated with methylbenzenethiol to provide a chemical background. Several regions along the collagen strand are marked. (b) Intensity of the collagen strand regions as a function of Raman shift using the tunable band-pass filter. A prominent peak around $\sim 1400$ cm$^{-1}$ is seen in these regions. (c) Image of the same region, this time with the band-pass filter tuned to enhance the background. (d) Intensity of several regions of the background as a function of Raman shift, this time showing peaks near $\sim 1000$, $\sim 1400$, $\sim 1600$, and $\sim 2500$ cm$^{-1}$. The $\sim 2500$ cm$^{-1}$ peak is unique to the thiol, so in this way, super-resolution chemical contrast imaging can be achieved with our plasmonic nanohole system.

fine split. Figure 3h was produced with rapidSTORM; the rest were produced with our homemade MATLAB code.[27] These results suggest that standard STORM algorithms may be used to accurately image nanohole arrays with minimal artifacts or plasmonic coupling effects. This may be due to the nanohole array not having a strong resonant grating order with the emitted Raman light. Measurements from the SEM image also show fiber widths to be $\sim 100$ nm, similar to the SERS-STORM image in Figure 2 and consistent with the literature.[41]

Other samples can also be imaged. For example, Figure 4 shows a chemical pattern of hexadecanethiol produced via microcontact printing techniques and soft lithography.[44] These chemical patterns were printed directly on our nanohole arrays and imaged in the same manner as Figure 3b. Figure 4a and b show the microcontact printing process. Briefly, a soft polydimethylsiloxane (PDMS) stamp is prepared[45] by using a silicon template (LightSmyth) consisting of 800 nm spaced lines. The PDMS was cured over the template and removed. This produced a stamp with an inverted pattern of the template. For microcontact printing[44] of chemical patterns, the surface of the stamp was coated with a solution of hexadecanethiol for 30 seconds before drying the excess liquid with compressed air. The PDMS stamp was then gently pressed to a nanohole array surface for 20 seconds and peeled away, leaving behind a chemical pattern. While the chemical pattern is not seen with a standard bright-field microscope image (Figure 4c), chemical contrast is shown when a SERS peak is imaged instead. A SERS spectrum of the surface was collected (Figure 4d), and a chemical image was formed by charting the intensity of a selected peak ($\sim 2500$ cm$^{-1}$, corresponding to the $\nu(\mathrm{SH})$ stretching mode) across the surface as the laser was scanned.

Figure 4e shows a clear stripe pattern produced by the PDMS stamp. This process was shown previously in a conference proceeding.[35] Here, to achieve subdiffraction-limited performance, we then used our SERS-STORM technique, shown in Figure 4f. While the chemical pattern itself has rather large (400 nm) line widths due to the PDMS stamp that was used, an improvement in resolution, sharpness, and details of the stripes is seen. Figure 4e and f are from two separate samples produced in an identical fashion, except Figure 4f was stamped with methylbenzenethiol. Other nonuniformities in the two images may be due to variations in the PDMS mold used for the microcontact printing process.

In Figure 5 we show full chemical contrast imaging. The images shown in Figures 2−4 were created either by monitoring a single band (e.g., at $\sim 1500$ cm$^{-1}$) of a diffraction-limited SERS signal or by monitoring the entire broadband signal at once for STORM. But to achieve chemical selectivity with our SERS-STORM imaging technique—as shown in the slow, diffraction-limited laser scanning mode of Figure 3b,c—it is important to capture the SERS spectrum. This can be done by using a tunable band-pass filter (Semrock, VersaChrome). By inserting the tunable band-pass filter before the EM-CCD, an image with a $\sim 10$ nm wide spectral band can be captured and then compiled. This sample contained a collagen fibril strand as well as a background layer of methylbenzenethiol. By taking 26 separate images, each at a different setting of the band-pass filter tuned from roughly 800 to 2600 cm$^{-1}$, a spectrum of the sample can be reconstructed. Figure 5a shows a SERS-STORM image of a collagen strand collected when the band-pass filter was tuned to $\sim 1400$ cm$^{-1}$, maximizing the contrast of the fiber. The microstructure of the
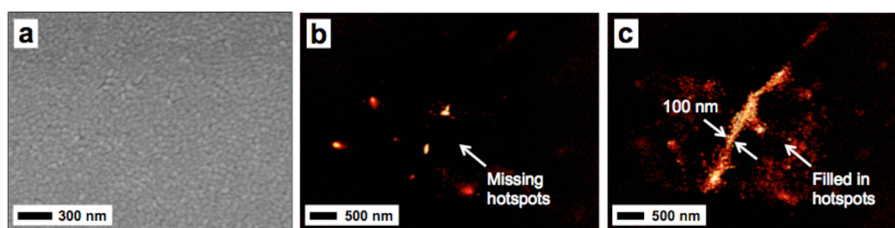
**Figure 6.** SERS-STORM imaging with an alternative substrate. (a) SEM image of a 10 nm thick, as-deposited silver film. Gaps and cracks are evident that will produce SERS hot spots in random locations. (b) SERS-STORM image of a short collagen strand on the randomly rough silver film. Some hot spots are seen, but there is no discernible structure. (c) By using our dynamic illumination technique to shift the locations of these hot spots, more features of the strand appear.

fiber is clearly resolved. The intensities of several regions (1, 2, and 3) in Figure 5a along the strand are monitored and produce a characteristic SERS spectrum. A prominent peak arising at $\sim$1400 cm$^{-1}$ is consistent with the literature for collagen.[41] At a different tuning of the band-pass filter, another image was recorded that enhanced the signal from the background, shown in Figure 5c. Plotting the intensity of three other regions (4, 5, and 6) in Figure 5d, several new, $\sim$1000, $\sim$1400, and $\sim$1600 cm$^{-1}$, peaks emerge that can be assigned to the benzene ring breathing mode, the $\nu$(HCH) bending mode of the methyl substituent, and the symmetric and asymmetric in-ring C−C=C bending modes, respectively. A third peak emerges at $\sim$2500 cm$^{-1}$ in all three regions and is distinct from the thiol $\nu$(SH) stretch. This enables the methylbenzenethiol to be discriminated from the collagen fibril. The strand in Figure 5 appears wider than those in Figures 2 and 3 perhaps due to imaging the methylbenzenethiol chemical background through the band-pass filter, increasing its apparent width. The spectral resolution (around 60−70 cm$^{-1}$) is due to the band-pass filter that was used and is not a limitation of the rest of the setup. These results show super-resolution SERS imaging of a sample region with chemical contrast.

Finally, the simplicity of using randomly varying illumination profiles to shift plasmonic hot spots and illuminate different regions of a nanohole array suggests that perhaps even a random SERS substrate could be used. To explore this possibility, Figure 6 shows an as-deposited, 10 nm thick rough silver film on a silicon substrate. The rough gaps, cracks, and grains of the silver are sufficient to excite SERS. We deposited collagen strands onto this sample as in Figures 2, 3, and 5. Figure 6b shows the SERS-STORM image with a uniform illumination beam. Clearly, the hot spot generation is nonuniform. Figure 6c shows the SERS-STORM image obtained by randomly altering the illumination profile as before with the SLM. More features of the strand appear, again showing fine details. Critically, the random nanotextured film also required our "dynamic" phase shifting of the plasmonic hot spots to "fill in the gaps". This shows that dynamic illumination (via an SLM or a simple optical diffuser) is important for super-resolution imaging on two very different plasmonic surfaces, opening up the door for more substrate optimization or alternative substrate designs.

We have shown plasmonic nanohole arrays and as-deposited silver films as super-resolution chemical imaging substrates using a SERS-STROM technique. Importantly, randomly varying the illumination profile via an optical diffuser was necessary to fill in the hot spot gaps that often plague SERS substrates. Comparison of our results to SEM images validated the SERS-STORM imaging technique. Finally, to show

chemical contrast, a tunable band-pass filter was inserted into the imaging path. These results show promise toward the development of a general-purpose platform capable of super-resolution, label-free chemical imaging of biological structures.

## ■ METHODS

A template stripping process was used to fabricate the nanohole array. The silicon template was first cleaned in a H$_2$O$_2$/H$_2$SO$_4$ (1:1) solution for 10 min and thoroughly washed with deionized water. Silver was then deposited onto the template at a rate of 30 nm/min using a thermal evaporator. To form clean, open nanoholes, the deposition needs to be at normal incidence. To strip the patterned silver from the template, a small drop of Norland 61 optical adhesive was used to adhere the silver to a clean glass microscope slide. The patterned silver was then stripped from the template. The 10 nm thick as-deposited silver films in Figure 6 were fabricated in a similar manner but used a smooth, unpatterned silicon chip. For several experiments, the nanoholes were submerged in a solution of 50 mM methylbenzene in ethanol for several hours or microcontact printed with a 50 mM methylbenzenethiol solution as described in the text. Collagen samples (derived from rat tail) were obtained from Sigma-Aldrich. To assemble the collagen into fibers for imaging, the powder was mixed to a concentration of 1 mg/mL in 20 mM acetic acid and then further diluted to 0.1 mg/mL in phosphate-buffered saline. After incubating in 37 °C water for 3 h, a small $\sim$0.1 mL portion of the polymerized solution was placed onto a fresh nanohole array chip, washed with deionized water, and then dried. The EM-CCD camera, spectrometer, and SLM were controlled with LabVIEW. Typical laser powers were 100 mW, although the SLM and the optical diffuser significantly reduced the available power at the sample to only a few mW. Imaging was performed on an inverted microscope with a 100×, 0.95 NA objective. For the scanning Raman imaging shown in Figure 3b, the laser was focused with the SLM to a tight diffraction-limited spot, and the microscope nanostage was programmed in LabVIEW to step in a 5-by-5 $\mu$m square. At each step, a SERS spectrum was recorded on the spectrometer (Horiba microHR) with an exposure time of 500 ms and saved with another custom LabVIEW program. For wide-field SERS-STORM imaging, integration times on the EMCCD were $\sim$100 ms. This exposure time allowed for observation of the blinking dynamics while at the same time giving sufficient signal-to-noise. For a typical imaging experiment, a movie of the blinking collagen strand or thiol pattern was recorded for several minutes on the EM-CCD. This video (a sample is shown in the Supporting Information) was then imported into rapid-STORM,[37] an open-source imaging platform that is capable of fast and efficient localization of the blinking events. After

some calibration (e.g., the image pixel size in nanometers and the diffraction-limited resolution of our microscope) a local threshold value was set via trial and error to obtain the cleanest SERS-STORM images with minimal background noise. We also imported the videos into a custom MATLAB script for image verification and obtained similar results (Figure 3e,f,g). The MATLAB script smoothed the video frames with a Gaussian convolution filter and found the position to within ~10 nm of all the local maxima above a certain threshold with a least-squares fit of a two-dimensional second-order polynomial. The positions of these hot spots were stored frame-by-frame and rendered as a final composite image. For more information about the sample preparation, optical setup, and imaging procedure, see our previous publication.[27] SEM imaging was performed with a Hitachi SU1510 tungsten SEM. An accelerating voltage of 5 kV was used to image the collagen strands on the nanohole arrays. To image the nanoholes separately or the as-deposited silver films, a higher accelerating voltage of 30 kV was used to resolve the fine details.

## ■ ASSOCIATED CONTENT

### Ⓢ Supporting Information

The Supporting Information is available free of charge on the ACS Publications website at DOI: 10.1021/acsphoto-nics.5b00647.

(PDF)

(AVI)

## ■ AUTHOR INFORMATION

### Corresponding Author

*E-mail: n-lindquist@bethel.edu; http://sites.google.com/a/bethel.edu/ncl48757-nanolab/.

### Notes

The authors declare no competing financial interest.
[†]Undergraduate students.

## ■ REFERENCES

(1) Hell, S. W. Far-field optical nanoscopy. *Science* **2007**, *316*, 1153−1158.

(2) Gustafsson, M. G. Extended resolution fluorescence microscopy. *Curr. Opin. Struct. Biol.* **1999**, *9*, 627−628.

(3) Betzig, E.; Trautman, J.; Harris, T.; Weiner, J.; Kostelak, R. Breaking the diffraction barrier: optical microscopy on a nanometric scale. *Science* **1991**, *251*, 1468−1470.

(4) Hell, S. W. Toward fluorescence nanoscopy. *Nat. Biotechnol.* **2003**, *21*, 1347−1355.

(5) Wang, P.; Slipchenko, M. N.; Mitchell, J.; Yang, C.; Potma, E. O.; Xu, X.; Cheng, J.-X. Far-field imaging of non-fluorescent species with subdiffraction resolution. *Nat. Photonics* **2013**, *7*, 449−453.

(6) Duponchel, L.; Milanfar, P.; Ruckebusch, C.; Huvenne, J.-P. Super-resolution and Raman chemical imaging: From multiple low

resolution images to a high resolution image. *Anal. Chim. Acta* **2008**, *607*, 168−175.

(7) Balzarotti, F.; Stefani, F. D. Plasmonics meets far-field optical nanoscopy. *ACS Nano* **2012**, *6*, 4580−4584.

(8) Barnes, W. L.; Dereux, A.; Ebbesen, T. W. Surface plasmon subwavelength optics. *Nature* **2003**, *424*, 824.

(9) Polman, A. Plasmonics Applied. *Science* **2008**, *322*, 868.

(10) Ozbay, E. Plasmonics: Merging photonics and electronics at nanoscale dimensions. *Science* **2006**, *311*, 189.

(11) Brolo, A. G. Plasmonics for future biosensors. *Nat. Photonics* **2012**, *6*, 709−713.

(12) Anker, J. N.; Hall, W. P.; Lyandres, O.; Shah, N. C.; Zhao, J.; Van Duyne, R. P. Biosensing with plasmonic nanosensors. *Nat. Mater.* **2008**, *7*, 442.

(13) Gordon, R.; Sinton, D.; Kavanagh, K. L.; Brolo, A. G. A new generation of sensors based on extraordinary optical transmission. *Acc. Chem. Res.* **2008**, *41*, 1049.

(14) Lindquist, N. C.; Lesuffleur, A.; Im, H.; Oh, S. H. Sub-micron resolution surface plasmon resonance imaging enabled by nanohole arrays with surrounding Bragg mirrors for enhanced sensitivity and isolation. *Lab Chip* **2009**, *9*, 382−387.

(15) Stiles, P. L.; Dieringer, J. A.; Shah, N. C.; Van Duyne, R. P. Surface-enhanced Raman spectroscopy. *Annu. Rev. Anal. Chem.* **2008**, *1*, 601.

(16) Stranahan, S. M.; Willets, K. A. Super-resolution optical imaging of single-molecule SERS hot spots. *Nano Lett.* **2010**, *10*, 3777−3784.

(17) Brolo, A. G.; Arctander, E.; Gordon, R.; Leathem, B.; Kavanagh, K. L. Nanohole-Enhanced Raman Scattering. *Nano Lett.* **2004**, *4*, 2015.

(18) Lesuffleur, A.; Kumar, L. K. S.; Brolo, A. G.; Kavanagh, K. L.; Gordon, R. Apex-enhanced Raman spectroscopy using double-hole arrays in a gold film. *J. Phys. Chem. C* **2007**, *111*, 2347.

(19) Bantz, K. C.; Meyer, A. F.; Wittenberg, N. J.; Im, H.; Kurtulus, Ö.; Lee, S. H.; Lindquist, N. C.; Oh, S. H.; Haynes, C. L. Recent progress in SERS biosensing. *Phys. Chem. Chem. Phys.* **2011**, *13*, 11551−11567.

(20) Lindquist, N. C.; Jose, J.; Cherukulappurath, S.; Chen, X.; Johnson, T. W.; Oh, S.-H. Tip-Based Plasmonics: Squeezing Light with Metallic Nanoprobes. *Laser Photonics Rev.* **2013**, *7*, 453.

(21) Juan, M. L.; Righini, M.; Quidant, R. Plasmon nano-optical tweezers. *Nat. Photonics* **2011**, *5*, 349.

(22) Righini, M.; Zelenina, A.; Girard, C.; Quidant, R. Parallel and selective trapping in a patterned plasmonic landscape. *Nat. Phys.* **2007**, *3*, 477.

(23) Weber, M. L.; Willets, K. A. Correlated Super-Resolution Optical and Structural Studies of Surface-Enhanced Raman Scattering Hot Spots in Silver Colloid Aggregates. *J. Phys. Chem. Lett.* **2011**, *2*, 1766−1770.

(24) Cang, H.; Labno, A.; Lu, C.; Yin, X.; Liu, M.; Gladden, C.; Liu, Y.; Zhang, X. Probing the electromagnetic field of a 15-nanometre hotspot by single molecule imaging. *Nature* **2011**, *469*, 385−388.

(25) Ayas, S.; Cinar, G.; Ozkan, A. D.; Soran, Z.; Ekiz, O.; Kocaay, D.; Tomak, A.; Toren, P.; Kaya, Y.; Tunc, I.; Zareie, H.; Tekinay, T.; Tekinay, A. B.; Begum; Guler, M. O.; Dana, A. Label-Free Nanometer-Resolution Imaging of Biological Architectures through Surface Enhanced Raman Scattering. *Sci. Rep.* **2013**, *3*, 2624.

(26) Willets, K. A. Super-resolution imaging of SERS hot spots. *Chem. Soc. Rev.* **2014**, *43*, 3854−3864.

(27) Ertsgaard, C. T.; McKoskey, R. M.; Rich, I. S.; Lindquist, N. C. Dynamic placement of plasmonic hotspots for super-resolution surface-enhanced Raman scattering. *ACS Nano* **2014**, *8*, 10941−10946.

(28) Olson, A. P., Ertsgaard, C. T., McKoskey, R. M., Rich, I. S., Lindquist, N. C. Super-resolution chemical imaging with dynamic placement of plasmonic hotspots, *Proc. SPIE* **2015**, *9554*, 95541410.1117/12.2188514.

(29) Gjonaj, B.; Aulbach, J.; Johnson, P. M.; Mosk, A. P.; Kuipers, L.; Lagendijk, A. Active spatial control of plasmonic fields. *Nat. Photonics* **2011**, *5*, 360−363.

(30) Kao, T.; Rogers, E.; Ou, J.; Zheludev, N. Digitally Addressable Focusing of Light into a Subwavelength Hot Spot. *Nano Lett.* **2012**, *12*, 2728−2731.

(31) Wei, F.; Liu, Z. Plasmonic Structured Illumination Microscopy. *Nano Lett.* **2010**, *10*, 2531.

(32) Ponsetto, J. L.; Wei, F.; Liu, Z. Localized plasmon assisted structured illumination microscopy for wide-field high-speed dispersion-independent super resolution imaging. *Nanoscale* **2014**, *6*, 5807−5812.

(33) Wei, F.; Lu, D.; Shen, H.; Wan, W.; Ponsetto, J. L.; Huang, E.; Liu, Z. Wide Field Super-Resolution Surface Imaging through Plasmonic Structured Illumination Microscopy. *Nano Lett.* **2014**, *14*, 4634−4639.

(34) Kim, K.; Oh, Y.; Lee, W.; Kim, D. Plasmonics-based spatially activated light microscopy for super-resolution imaging of molecular fluorescence. *Opt. Lett.* **2010**, *35*, 3501.

(35) Elliott, S. N., Turner, M. A., Rich, I. S., Lindquist, N. C. Fabrication and Characterization of Template-Stripped Plasmonic Substrates for High-Resolution Chemical Imaging, *CLEO: 2014, OSA Technical Digest* (online), paper JTu4A.12, 2014.

(36) Rust, M. J.; Bates, M.; Zhuang, X. Sub-diffraction-limit imaging by stochastic optical reconstruction microscopy (STORM). *Nat. Methods* **2006**, *3*, 793−796.

(37) Wolter, S.; Löschberger, A.; Holm, T.; Aufmkolk, S.; Dabauvalle, M.-C.; van de Linde, S.; Sauer, M. rapidSTORM: accurate, fast open-source software for localization microscopy. *Nat. Methods* **2012**, *9*, 1040−1041.

(38) Ebbesen, T. W.; Lezec, H. J.; Ghaemi, H. F.; Thio, T.; Wolff, P. A. Extraordinary optical transmission through sub-wavelength hole arrays. *Nature* **1998**, *391*, 667.

(39) Liu, L. Z.; O'Keeffe, K.; Lloyd, D. T.; Hooker, S. M. General analytic solution for far-field phase and amplitude control, with a phase-only spatial light modulator. *Opt. Lett.* **2014**, *39*, 2137−2140.

(40) Nagpal, P.; Lindquist, N. C.; Oh, S. H.; Norris, D. J. Ultrasmooth patterned metals for plasmonics and metamaterials. *Science* **2009**, *325*, 594.

(41) Gullekson, C.; Lucas, L.; Hewitt, K.; Kreplak, L. Surface Enhanced Raman Spectroscopy of Collagen I Fibrils. *Biophys. J.* **2011**, *100*, 1837.

(42) Gustafsson, M. G. L. Surpassing the lateral resolution limit by a factor of two using structured illumination microscopy. *J. Microsc.* **2000**, *198*, 82−87.

(43) Willets, K. A. Super-resolution imaging of interactions between molecules and plasmonic nanostructures. *Phys. Chem. Chem. Phys.* **2013**, *15*, 5345−5354.

(44) Gates, B. D.; Xu, Q.; Stewart, M.; Ryan, D.; Willson, C. G.; Whitesides, G. M. New approaches to nanofabrication: molding, printing, and other techniques. *Chem. Rev.* **2005**, *105*, 1171.

(45) Xia, Y.; Whitesides, G. M. Soft lithography. *Annu. Rev. Mater. Sci.* **1998**, *28*, 153−184.